



**HAL**  
open science

## Synthesis and Crystal Structures of $\text{InGaO}_3(\text{ZnO})_m$ ( $m = 2$ and $3$ )

Isabelle Keller, Wilfried Assenmacher, Gregor Schnakenburg, Werner Mader

► **To cite this version:**

Isabelle Keller, Wilfried Assenmacher, Gregor Schnakenburg, Werner Mader. Synthesis and Crystal Structures of  $\text{InGaO}_3(\text{ZnO})_m$  ( $m = 2$  and  $3$ ). *Journal of Inorganic and General Chemistry / Zeitschrift für anorganische und allgemeine Chemie*, 2009, 635 (12), pp.2065. 10.1002/zaac.200900199. hal-00509230

**HAL Id: hal-00509230**

**<https://hal.science/hal-00509230>**

Submitted on 11 Aug 2010

**HAL** is a multi-disciplinary open access archive for the deposit and dissemination of scientific research documents, whether they are published or not. The documents may come from teaching and research institutions in France or abroad, or from public or private research centers.

L'archive ouverte pluridisciplinaire **HAL**, est destinée au dépôt et à la diffusion de documents scientifiques de niveau recherche, publiés ou non, émanant des établissements d'enseignement et de recherche français ou étrangers, des laboratoires publics ou privés.



### Synthesis and Crystal Structures of $\text{InGaO}_3(\text{ZnO})_m$ ( $m = 2$ and 3)

Journal:	<i>Zeitschrift für Anorganische und Allgemeine Chemie</i>
Manuscript ID:	zaac.200900199.R1
Wiley - Manuscript type:	Article
Date Submitted by the Author:	29-May-2009
Complete List of Authors:	Keller, Isabelle; Universität Bonn, Institut für Anorganische Chemie Assenmacher, Wilfried; Universität Bonn, Institut für Anorganische Chemie Schnakenburg, Gregor; Universität Bonn, Institut für Anorganische Chemie Mader, Werner; University of Bonn, Chemistry
Keywords:	Indium gallium zinc oxides, Flux synthesis, Electron diffraction, Crystal structures



## ARTICLE

DOI: 10.1002/zaac.200((will be filled in by the editorial staff))

Synthesis and Crystal Structures of  $\text{InGaO}_3(\text{ZnO})_m$  ( $m = 2$  and  $3$ )Isabelle Keller,<sup>[a]</sup> Wilfried Assenmacher,<sup>[a]</sup> Gregor Schnakenburg,<sup>[a]</sup> and Werner Mader<sup>\*[a]</sup>*Dedicated to Prof. Dr. Dr. h. c. Martin Jansen on the Occasion of his 65<sup>th</sup> Birthday***Keywords:** Indium gallium zinc oxides; Flux synthesis; Electron diffraction; Crystal structures

An optimized high temperature route in sealed platinum tubes was used for synthesis of pure powders of members of the homologues series  $\text{InGaO}_3(\text{ZnO})_m$ . Single crystals of  $\text{InGaO}_3(\text{ZnO})_2$  were grown from a  $\text{K}_2\text{MoO}_4$  flux.  $\text{InGaO}_3(\text{ZnO})_2$  crystallises in the hexagonal crystal system ( $P6_3/mmc$ ; No. 194), deduced from convergent beam electron diffraction (CBED). Single crystal structure refinement from XRD data ( $a = 3.2909(2)$  Å;  $c = 22.485(2)$  Å;  $Z = 2$ ; 1603 data,  $R1 = 0.0237$ ) revealed a compound which consist of an alternate stacking of  $[\text{InO}_{6/3}]_2^{\infty}$  and  $[(\text{Ga,Zn})\text{O}_{4/4}]_3^{\infty}$  corresponding to  $\text{CdI}_2$  and wurtzite type structure motifs, respectively. Inversions of the  $\text{ZnO}_4$  tetrahedra occurs (i) at the  $\text{InO}_6$  octahedral layer and (ii) halfway in the wurtzite type region where the inversion boundary is built by  $\text{Ga}^{3+}$  in trigonal bipyramidal co-ordination with a long Ga-O<sub>apical</sub> distance of 2.138 Å.

The site occupation of  $\text{Zn}^{2+}$  and  $\text{Ga}^{3+}$ , respectively, was confirmed by valence sum calculations. The structure of  $\text{InGaO}_3(\text{ZnO})_3$  was refined from powder X-ray diffraction data.  $\text{InGaO}_3(\text{ZnO})_3$  crystallises trigonal ( $R\bar{3}m$ ; No. 166;  $a = 3.2871(9)$  Å;  $c = 41.589(1)$  Å,  $R_{\text{Bragg}} = 0.0506$ ). The space group was confirmed by CBED. The structure of  $\text{InGaO}_3(\text{ZnO})_3$  is similar to  $\text{InGaO}_3(\text{ZnO})_2$ , however, the wurtzite type part of the structure has an even number of closed packed oxygen layers and thus the inversion boundary within this area is different. The compounds described here have the structural characteristics as other known members with general formula  $(\text{ARO}_3)\cdot(\text{ZnO})_m$  with  $m = \text{integer}$ .

\* Prof. Dr. W. Mader

Fax: +49-288-734205

E-mail: mader@uni-bonn.de

[a] Institut für Anorganische Chemie, Universität Bonn,  
Römerstrasse 164  
53117 Bonn, Germany**Introduction**

ZnO has unique optical, electronic and piezoelectric properties and is therefore used for various applications such as phosphors, varistors and mechanical transducers. [1-7]. The reaction of ZnO with oxides of trivalent ions (sesqui oxides) leads to compounds with unusual structural characteristics and improved properties for electronic [8] or thermoelectric applications [1]. The general formula of such mixed oxides is  $\text{ARO}_3(\text{ZnO})_m$  ( $m = \text{integer}$ ; A, R = trivalent ions). Several homologous compounds of oxides of  $\text{ARO}_3(\text{MO})_m$  ( $M = \text{Mg, Mn, Fe, Co, Cu, Zn, Cd}$ ;  $A = \text{Sc, Y, In, Ho, Er, Tm, Yb, Lu}$ ;  $R = \text{Al, Fe, Ga}$ ) are described [9-13]. Aristotypes for this series of compounds are  $\text{YbFe}_2\text{O}_4$  ( $=\text{FeYbO}_3(\text{FeO})_1$ ) [14] and  $\text{In}_2\text{ZnS}_4$  ( $=\text{In}_2\text{S}_3(\text{ZnS})_1$ ) [15], respectively. The anions in these compounds are in a closest-packed arrangement. Within this packing one of the trivalent ions occupies octahedral interstices, forming layers of edge sharing octahedra  $[\text{AO}_{6/3}]_2^{\infty}$ . In between these layers are regions of variable size with composition  $[\text{M}_m\text{RO}_{m+1}]^+$  and having a wurtzite type of structure  $[(\text{M,R})\text{O}_{4/4}]_3^{\infty}$ . The structures exhibit two alternating inversion boundaries. The  $(\text{M,R})\text{O}_4$  tetrahedra are connected via corners to the

octahedral layers, hence the two wurtzite blocks facing an octahedral layer are inverted. To fulfil this condition at any octahedral layer, a second inversion inside the wurtzite block has to exist. It is proposed that these compounds crystallise in the space group  $R\bar{3}m$  for  $m = \text{odd}$  and  $P6_3/mmc$  for  $m = \text{even}$ , respectively [16]. Structural details from single crystal X-ray diffraction are known of only few compounds. Furthermore, it is difficult to synthesize pure compounds [10]. In many studies it is reported that mixtures of phases with  $m \pm 1$  were obtained [9].

In the present contribution, we report about the synthesis and structural characterisation of compounds in the  $\text{ZnO} - \text{In}_2\text{O}_3 - \text{Ga}_2\text{O}_3$  system. The compound  $\text{InGaO}_3(\text{ZnO})_2$  could be obtained as single crystals, and to our knowledge it is the second single crystal study of such homologous compounds apart of  $\text{LuFeO}_3(\text{ZnO})_m$  ( $m = 1, 4 - 6$ ) reported by Isobe et al. [16, 17]. In our study we were even able to locate the cation sites in the wurtzite block by X-ray diffraction and bond valence calculations. Furthermore, details such as anisotropic displacements of ions in the inversion boundary inside the wurtzite block could be observed and are discussed. We also deduced the structure of the compound  $\text{InGaO}_3(\text{ZnO})_3$  from powder data by Rietveld refinement. With these new results we gain insight into these compounds, in particular into the ordering within the wurtzite type region. Additionally, to verify the reported space groups of the two compounds, the structures were analysed using convergent beam electron diffraction (CBED).

## Experimental Section

In<sub>2</sub>O<sub>3</sub> (99.999 %, Alfa Aesar), Ga<sub>2</sub>O<sub>3</sub> (99.999 %, Alfa Aesar) and ZnO (99.999 %, Alfa Aesar) were used as purchased, without further purification. Calculated amounts of the starting compounds were weighed and thoroughly mixed in an agate mortar dispersed in acetone. After drying, the powder mixtures were pressed to pellets and sealed in Pt tubes. Single phase polycrystalline samples were obtained by heating the pellets twice at 1623 K for 3 days, interrupted for homogenisation by grinding. This material was used for powder X-ray diffraction studies and for transmission electron microscopy (TEM). Single crystals were grown in a K<sub>2</sub>MoO<sub>4</sub> flux. For this purpose, potassium molybdate (98 %, Aldrich) was added to the mixture of the starting oxides at an excess ratio of 20:1 in weight. The mixture was annealed in a sealed Pt tube for 5 days at 1623 K and cooled at a rate of 0.1 K/min to 873 K. Thus, colourless single crystals of InGaO<sub>3</sub>(ZnO)<sub>2</sub> were obtained and were isolated from the molybdate by washing with warm (70 °C) distilled water.

Electron diffraction was conducted on transmission electron microscopes FEI-Philips CM300 UT/FEG and FEI-Philips CM30 T/LaB<sub>6</sub>, operated at 300 kV. Convergent beam electron diffraction (CBED) patterns were acquired without inelastically scattered electrons using a post column electron energy imaging filter (Gatan GIF) attached to the CM300 electron microscope.

A scanning electron microscope Zeiss-LEO Supra55 FEG-SEM equipped with an Oxford energy dispersive X-ray spectrometry (EDXS) system was used for imaging single crystals and for chemical microanalysis. Powder X-ray diffraction data were obtained on a digitised Philips PW1050 (Co K<sub>α</sub> radiation), Bragg-Brentano geometry, and post specimen monochromator. X-ray diffraction data of single crystals were collected on a Kappa-CCD-diffractometer (Bruker-Nonius) with Mo K<sub>α1</sub> radiation.

## Results and Discussion

### Space group determination by electron diffraction and convergent beam electron diffraction (CBED)

#### InGaO<sub>3</sub>(ZnO)<sub>2</sub>

Selected area electron diffraction (SAED) patterns of InGaO<sub>3</sub>(ZnO)<sub>2</sub> in the zone axes [2;<sup>-</sup>110], [011;<sup>-</sup>0] and [0001] as well as a CBED pattern in [0001] are shown in Fig. 1. The electron diffraction patterns can be indexed in a hexagonal crystal system with unit cell parameters  $a_0 = 3.30$  Å and  $c_0 = 22.74$  Å. The diffraction conditions are  $(2;<sup>-</sup>h;<sup>-</sup>h)l: l = 2n$  (Fig. 1b) which result in the possible space groups  $P6_3mc$  (No. 186),  $P6_3c$  (No. 190) and  $P6_3/mmc$  (No. 194). In the [2;<sup>-</sup>110] pattern (Fig. 1a) this information is not available due to dynamic double diffraction.

The method of CBED is known for determination of the space group of a crystal since the whole crystal contributes to the diffraction pattern. The CBED pattern in the [0001] zone axis (Fig. 1d) exhibits  $6mm$  whole-pattern symmetry as well as  $6mm$  symmetry in the bright field disc (Fig. 1e). According to Morniroli & Steeds [18] two hexagonal space groups are remaining:  $P6_3mc$  and  $P6_3/mmc$ . The number of independent mirror planes decides the space group, i.e.  $2mm$  or  $2m$  point group symmetry, respectively. These two symmetries can be discriminated from electron diffraction patterns having reflections of higher order Laue zones [19]. Starting in the [011;<sup>-</sup>0] zone axis orientation (Fig. 2a), the crystal was tilted towards the  $c$  axis. The corresponding

diffraction pattern (Fig. 2b) shows mirror symmetry in all details proving the prism planes of type  $\{2;<sup>-</sup>110\}$  to be mirror planes ( $m_1$ ) of the crystal. Tilting the crystal out of [011;<sup>-</sup>0] perpendicular to the  $c$  axis yields the diffraction pattern in Fig. 2c which shows mirror symmetry perpendicular to  $m_1$ . This second mirror plane ( $m_2$ ) is parallel to the basal plane of the crystal. As a result, InGaO<sub>3</sub>(ZnO)<sub>2</sub> crystallises in space group  $P6_3/mmc$  (No. 194).

#### InGaO<sub>3</sub>(ZnO)<sub>3</sub>

Electron diffraction patterns of InGaO<sub>3</sub>(ZnO)<sub>3</sub> are displayed in Fig. 3 and Fig. 4. The [0001] zone axis CBED whole pattern (Fig. 3d) as well as the central CBED disc (Fig. 4a) exhibit three-fold symmetry, proving a trigonal crystal system. The SAED patterns (Fig. 3 a-c) can be indexed using a unit cell with hexagonal axes  $a_0 = 2.90$  Å and  $c_0 = 43.07$  Å. The diffraction conditions are  $hkl: -h + k + l = 3n$ ,  $hh;<sup>-</sup>0l: h + l = 3n$ ,  $hh(2;<sup>-</sup>h;<sup>-</sup>l): l = 3n$  and  $000l: l = 3n$ , which leads to the possible spacegroups  $R3$  (No. 146),  $R3;<sup>-</sup>$  (No. 148),  $R32$  (No. 155),  $R3m$  (No. 160) and  $R3;<sup>-</sup>m$  (No. 166). Close inspection of the CBED patterns clearly show  $3m$  pattern symmetry. Therefore, only the two space groups  $R3m$  and  $R3;<sup>-</sup>m$  are possible. Finally, the six-fold symmetry of the diffraction pattern of the zero order Laue zone (ZOLZ), seen to be present in Fig. 3c, yields the space group  $R3;<sup>-</sup>m$  [19]. Moreover, the CBED pattern simulated with the EMS computer code [20] using the InGaO<sub>3</sub>(ZnO)<sub>3</sub> structure data from powder diffraction shows an excellent agreement with the experimental CBED pattern (Fig. 4).

### Crystal structure of InGaO<sub>3</sub>(ZnO)<sub>2</sub> from single crystal X-ray diffraction

Suitable single crystals of InGaO<sub>3</sub>(ZnO)<sub>2</sub> for structure determination were chosen using a light microscope with polarizer. A scanning electron micrograph of a InGaO<sub>3</sub>(ZnO)<sub>2</sub> crystal is shown in Fig. 5. The chemical composition of the crystal was confirmed by EDXS resulting in the ratio of metal ions Zn:Ga:In = 50.07: 24.38: 25.55 with an error less than ±1 each. The observed reflection conditions of InGaO<sub>3</sub>(ZnO)<sub>2</sub> were found to be consistent with the hexagonal space group  $P6_3/mmc$ , which was also determined by electron diffraction. The crystal structure was solved by direct methods [21] and refined against  $F^2$  [21]. In the first structure solution all cation positions were determined. The positions of the oxygen ions were found by difference fourier synthesis. Crystal and refinement parameters are summarised in table 1 and atomic coordinates and displacement parameters are given in table 2.

The result shows that InGaO<sub>3</sub>(ZnO)<sub>2</sub> is a member of the structure family with general formula  $ARO_3(ZnO)_m$ . The larger trivalent ion (In<sup>3+</sup>) is octahedrally coordinated by oxygen with an octahedron slightly compressed in the direction of the  $c$  axis. The InO<sub>6</sub> octahedra are connected by sharing edges to form layers parallel to the basal plane. Zn<sup>2+</sup> has a slightly distorted tetrahedral co-ordination. The ZnO<sub>4</sub> tetrahedra share corners at both sides to a  $[InO_{6/3}]_b^c$  layer. This configuration has to exist at any octahedral layer which implies another inversion boundary to exist. This inversion plane is built by Ga<sup>3+</sup> ions in trigonal bipyramidal co-ordination in the wurtzite type block at half distance

between the layers of  $\text{InO}_6$  octahedra (Fig. 6a). The distance between  $\text{Ga}^{3+}$  and the apical  $\text{O}^{2-}$  ions amounts to 2.137 Å and is hence unexpectedly large and much longer than the distance of 1.900(1) Å between Ga and the equatorial oxygen ions. There is only one example of such a long Ga-O distance in literature observed in  $\text{GaO}_3(\text{PO}_4)$  where Ga has a trigonal bipyramidal coordination as well [22]. The  $\text{GaO}_5$  polyhedra share corners among each other and with neighbouring  $\text{ZnO}_4$  units, respectively. The displacement parameter of O3, the oxygen ion in the equatorial plane of the  $\text{GaO}_5$  unit, is somewhat elongated along  $c$ , which may indicate a split position. Attempts to refine a split position for this O atom showed no reasonable results. Alternatively, the structure may be regarded in terms of closed-packed spheres with oxygen ions being closed-packed.  $\text{In}^{3+}$  ions occupy octahedral sites forming a layer structure with composition  $[\text{InO}_2]$ , comparable with the  $\text{CdI}_2$  type of structure. These layers are connected via corners with the wurtzite structure motifs having the composition  $[(\text{GaZn}_2)\text{O}_3]^+$ . The change of  $\text{Zn}^{2+}$  site occupation from  $\text{T}^+$  to  $\text{T}^-$  positions (inversion of the wurtzite structure) is realised by filling trigonal bipyramidal sites with  $\text{Ga}^{3+}$ , which may be regarded as bitetrahedra. The stacking sequence of the closed-packed oxygen layers changes from ABAB.. to ACAC.. at the  $[\text{InO}_{6/3}]_b^+$  layers. Thus there is a cubic stacking of the closed-packed layers with In in octahedral sites.

$\text{Zn}^{2+}$  and  $\text{Ga}^{3+}$  are isoelectronic and thus indistinguishable by X-ray diffraction. Calculations of bond valence sums by the program softBV0.96 [23, 24] helped to differentiate between Zn and Ga. The calculation of the bond valence sum was reasonable only with Zn in tetrahedral sites and Ga in trigonal bipyramidal interstices.

Atomic distances and angles in each coordination polyhedron (see Fig. 6 b-d) are listed in table 3. The compression of the  $\text{InO}_6$  octahedra yields O-In-O bond angles which deviate by  $10^\circ$  from the ideal  $90^\circ$  angle.

In the  $\text{GaO}_5$  trigonal bipyramid the long distances of gallium to the apical O2 ions [Ga-O2: 2.1379(2) Å; Table 3] are the result of the position of the gallium in the equatorial triangle of the trigonal bipyramid. The  $\text{Zn}^{2+}$  ion is shifted off the centre of the  $\text{ZnO}_4$  tetrahedron along  $c$  towards the trigonal bipyramid which increases the angle O2-Zn-O2 with respect to O1-Zn-O2.

### Crystal structure of $\text{InGaO}_3(\text{ZnO})_3$ from powder X-ray diffraction

The crystal structure of  $\text{InGaO}_3(\text{ZnO})_3$  was refined from powder X-ray diffracton data shown in Fig. 7. Structure data of  $\text{LuFeO}_3(\text{ZnO})_3$  [16] were used as starting model for the refinement. After a first refinement, the structure model was validated by bond valence calculations concerning the  $\text{Ga}^{3+}$  distribution. These calculations favoured a model with  $\text{Ga}^{3+}$  only in the tetrahedra at the inversion plane within the wurtzite region. Thus, these tetrahedra are statistically occupied by Zn and Ga, whereas the tetrahedra linked to the layers of  $\text{InO}_6$  octahedra are occupied by Zn only. Only two weak reflections at ca.  $18^\circ$  and  $29^\circ$   $2\theta$  could not be assigned to the pattern of  $\text{InGaO}_3(\text{ZnO})_3$ . The displacement parameter for the oxygen atom O1 could not be refined anisotropically. The results and  $R$  values for  $\text{InGaO}_3(\text{ZnO})_3$  are given in table 4.

The structure of  $\text{InGaO}_3(\text{ZnO})_3$  is displayed in Fig. 8, and it is assembled similarly as the structure of  $\text{InGaO}_3(\text{ZnO})_2$ . In a close packing of oxygen ions  $\text{In}^{3+}$  occupies octahedral sites forming  $[\text{InO}_{6/3}]_b^+$  layers. These layers are parallel to the basal plane and are separated by wurtzite type regions  $[(\text{GaZn}_3)\text{O}_4]^+$  of  $\text{ZnO}_4$  and  $(\text{Zn,Ga})\text{O}_4$  tetrahedra, respectively. According to the composition, the thickness of the wurtzite type region is larger than in  $\text{InGaO}_3(\text{ZnO})_2$  by one additional close packed oxygen layer and hence one additional tetrahedrally coordinated cation position. The inversion plane in the centre of the  $[(\text{GaZn}_3)\text{O}_4]^+$  region lies between two  $(\text{Zn,Ga})\text{O}_4$  tetrahedra, because of the number of oxygen layers is even.

Again, the cation is shifted from the tetrahedron center towards the basal plane with increasing distance from the  $\text{InO}_6$  octahedral layer. Thus, the distance between the cation and the apical oxygen ion increases from 1.8981 Å for Zn1-O1 to 2.0395 for (Zn2,Ga2)-O2 and the distance to the basal oxygen decreases, respectively (Fig. 8b and 8c).

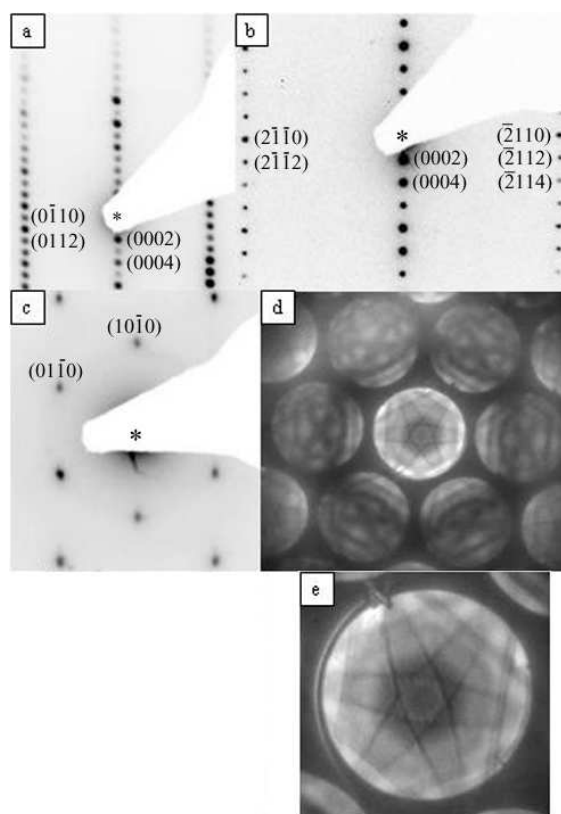


Figure 1. Electron diffraction patterns of  $\text{InGaO}_3(\text{ZnO})_3$  along zone axes (a)  $[011; \bar{0}]$ , (b)  $[2; \bar{1}10]$ , and (c)  $[0001]$ , and CBED pattern in the  $[0001]$  zone axis (d). Whole pattern (d) and bright field CBED disc (e) exhibit hexagonal symmetry. Forbidden weak reflections  $000l$  ( $l = 2n+1$ ) in (a) is the result of dynamic electron scattering.

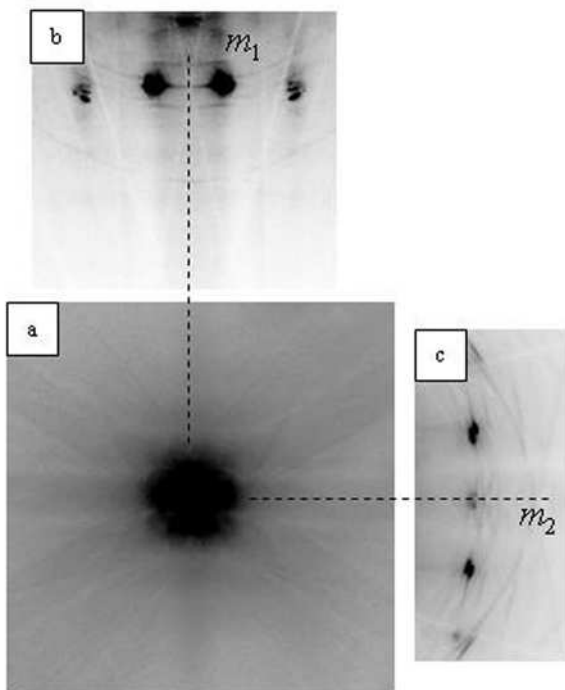


Figure 2. (a)  $[011;\bar{0}]$  zone axis of the  $\text{InGaO}_3(\text{ZnO})_2$  compound, (b) diffraction pattern after crystal tilt along  $m_1$  mirror plane, (c) diffraction pattern after crystal tilt along  $m_2$  mirror plane.

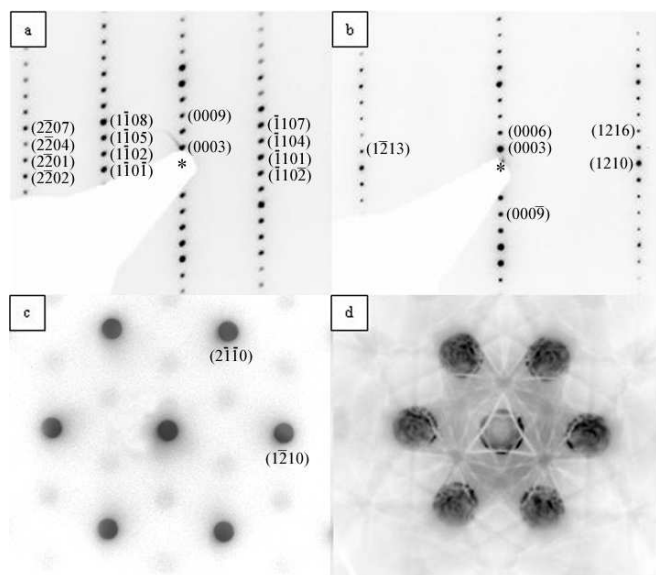


Figure 3. Electron diffraction patterns of  $\text{InGaO}_3(\text{ZnO})_3$  along (a)  $[112;\bar{0}]$ , (b)  $[101;\bar{0}]$ , and (c)  $[0001]$ . (d) The CBED pattern is in the  $[0001]$  zone axis. Weak reflections in (c) are in the Laue zones  $l = +1$  and  $l = -2$ .

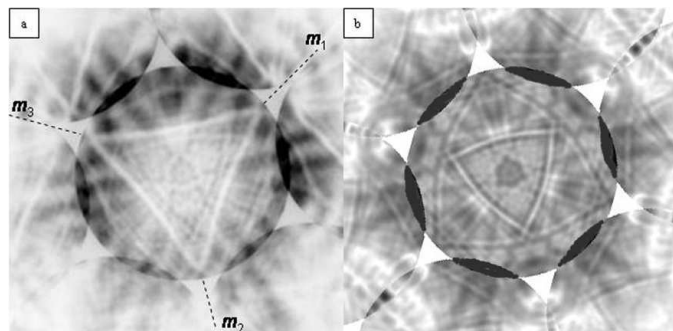


Figure 4. Experimental (a) and computer simulated (b) CBED central disc in  $[0001]$  zone axis. The two discs exhibit  $3m$  symmetry. The simulated CBED disc confirms space group  $R\bar{3}m$ .

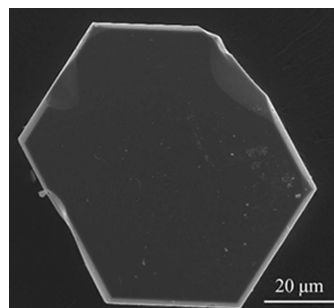


Figure 5. SEM image of a single crystal of  $\text{InGaO}_3(\text{ZnO})_2$ .

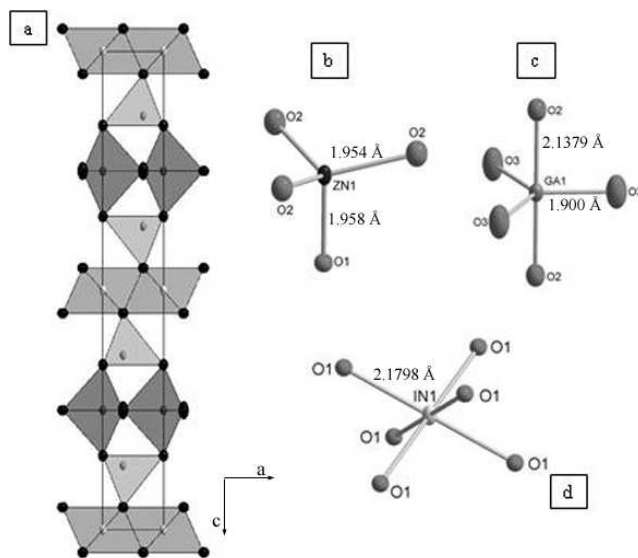


Figure 6. Structure of  $\text{InGaO}_3(\text{ZnO})_2$  viewed along  $a$ , (a). Coordination of  $\text{Zn}^{2+}$  (b),  $\text{Ga}^{3+}$  (c), and  $\text{In}^{3+}$  (d). Thermal displacement parameters at 90 % probability.

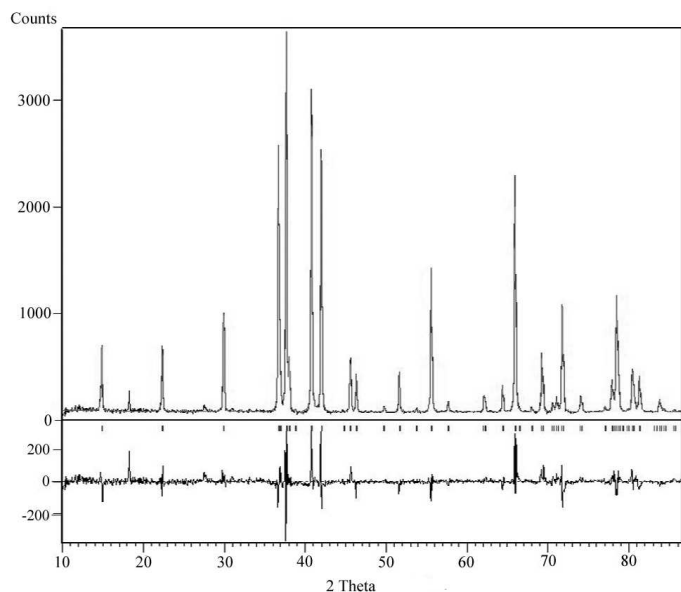


Figure 7. Experimental and calculated powder X-ray diffraction patterns and the corresponding difference plot for  $\text{InGaO}_3(\text{ZnO})_3$ .

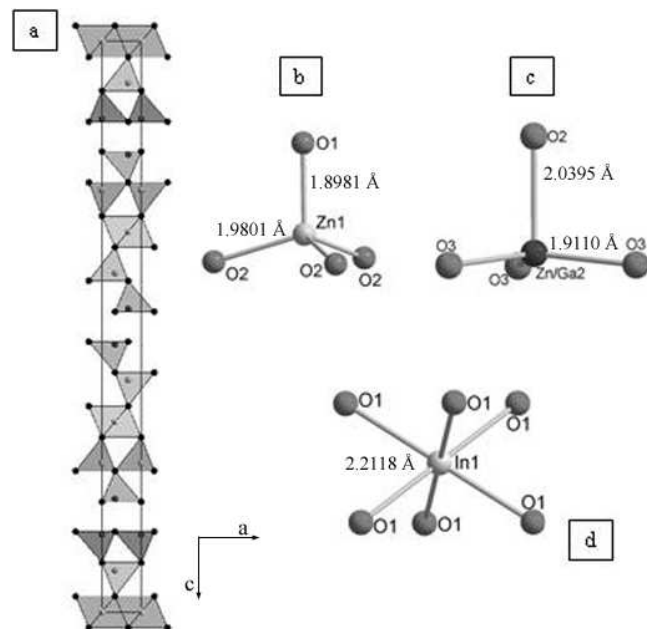


Figure 8. Structure of  $\text{InGaO}_3(\text{ZnO})_3$  viewed along  $a$  (a). Coordination of  $\text{Zn}1$  (b), of  $\text{Zn}/\text{Ga}2$  (c), and of  $\text{In}1$  (d).

Table 1 Crystal data and refinement results of  $\text{InGaO}_3(\text{ZnO})_2$ .

Empirical formula	$\text{GaInZn}_2\text{O}_5$
Formula weight	395.28 g/mol
Space group	$P6_3/mmc$ (No. 194)
Unit cell dimensions	$a = 3.2909(2) \text{ \AA}$ $c = 22.485(2) \text{ \AA}$
Volume	$210.89(3) \text{ \AA}^3$
No. of formula units per unit cell	2
Calculated density	$6.225 \text{ g/cm}^3$
Crystal size	$0.24 \times 0.21 \times 0.04 \text{ mm}^3$
Crystal colour	colourless
T	123 K
Absorption correction type	numerical
Absorption coefficient	$22.868 \text{ mm}^{-1}$
$F(000)$	360.00
$\circ$ range for data collection	$5.44\text{--}34.91$
Index ranges	$-4 \leq h \leq 4$ $-4 \leq k \leq 5$ $-29 \leq l \leq 36$
Reflections collected	1603
Independent reflections	224 (Rint = 0.057)
Refinement method	Full-matrix least-square on $F^2$
Goodness of fit on $F^2$	1.432
Final $R$ indices [ $I > 2\sigma(I)$ ]	$R1 = 0.0237$ , $wR2 = 0.0711$
Extinction coefficient	0.028172
Largest diff. Peak and hole $\times 10^{-3}$	1.81 and $-1.46 \text{ e/nm}^3$

Table 2a Atomic coordinates and  $U_{eq}$  of  $\text{InGaO}_3(\text{ZnO})_2$ .

Atom	Position	$x$	$y$	$z$	sof	$U_{eq} / \text{\AA}^2$
In1	24	0.00000	0.00000	0.00000	1	0.0059(2)
Zn1	4f	0.66667	0.33333	0.36538(5)	1	0.0051(3)
Ga1	2b	0.00000	0.00000	0.25000	1	0.0061(3)
O1	4f	0.66667	0.33333	0.4525(3)	1	0.006(1)
O2	4e	1.00000	0.00000	0.3451(3)	1	0.010(1)
O3	2d	-0.33333	0.33333	0.25000	1	0.016(2)

Table 2b Anisotropic displacement parameters ( $\text{\AA}^2$ ) of  $\text{InGaO}_3(\text{ZnO})_2$ .

Atom	<i>U</i> 11	<i>U</i> 22	<i>U</i> 33	<i>U</i> 23	<i>U</i> 13	<i>U</i> 12
In1	0.0044(3)	0.0044(3)	0.0087(4)	0.00000	0.00000	0.0022(1)
Zn1	0.0037(3)	0.0037(3)	0.078(4)	0.00000	0.00000	0.0018(1)
Ga1	0.0048(4)	0.0048(4)	0.087(6)	0.00000	0.00000	0.0024(2)
O1	0.006(1)	0.006(1)	0.006(2)	0.00000	0.00000	0.0031(7)
O2	0.009(2)	0.009(2)	0.012(3)	0.00000	0.00000	0.0045(9)
O3	0.009(5)	0.009(5)	0.031(5)	0.00000	0.00000	0.004(1)

Table 4 Crystal data and rietveld refinement of the  $\text{InGaO}_3(\text{ZnO})_3$  compound.

Radiation	Co K $\alpha$
Empirical formula	$\text{GaInZn}_3\text{O}_6$
Formula weight	1430.03 g/mol
Space group	<i>R</i> -3 <i>m</i> (No. 166)
Unit cell dimensions	<i>a</i> = 328.971(9) pm <i>c</i> = 4158.9(1) pm
Volume	389.788 $\text{\AA}^3$
Number of formula units per unit cell	3
Calculated density	6.09 g/cm $^3$
F(000)	654.00
Colour of the microcrystalline powder	yellow
Number of free parameters	29
Profile function	Pseudo-Voigt
<i>R</i> <sub>Bragg</sub> /%	5.057
<i>R</i> <sub>p</sub> /%	9.218
Gof / %	2.201

Table 3 Bond lengths ( $\text{\AA}$ ) and angles ( $^\circ$ ) of  $\text{InGaO}_3(\text{ZnO})_2$ .

In1	O1	O2	O3
O1	<b>2.1798(1)</b>	3.0727(2)	4.5527(4)
O2		3.4833(3)	2.8580(2)
O3			5.9336(5)

Zn1	O1	O2	O3
O1	<b>1.9584(2)</b>	3.0727(2)	4.5527(4)
O2		<b>1.9540(1)</b>	2.8580(2)
O3			2.5943(2)

Ga1	O1	O2	O3
O1	4.9333(4)	3.0727(2)	4.5527(4)
O2		<b>2.1379(2)</b>	2.8580(2)
O3			<b>1.9000(1)</b>

$\angle$ (O1, In1, O1)	$\angle$ (O1, Zn1, O2)	$\angle$ (O2, Zn1, O2)
98.027(1)	103.507(2)	114.719(1)

$\angle$ (O2, Ga1, O3)	$\angle$ (O3, Ga1, O3)
90	120

Table 5 Atomic coordinates, occupancy, and isotropic displacement parameters B of  $\text{InGaO}_3(\text{ZnO})_3$ .

Atom	Wyck.	sof not refined	<i>x</i>	<i>y</i>	<i>z</i>	B/ $\text{\AA}^2$
In1	3a	1	0	0	0	2.39(5)
Zn1	6c	1	0	0	0.73956(9)	2.16(5)
Ga2	6c	0.5	0	0	0.13539(9)	2.34(5)
Zn2	6c	0.5	0	0	0.13539(9)	2.34(5)
O1	6c	1	0	0	0.3061(4)	3.3(5)
O2	6c	1	0	0	0.0864(3)	0.5(2)
O3	6c	1	0	0	0.8071(3)	1.5(2)

## Conclusions

Members of the homologous series  $\text{InGaO}_3(\text{ZnO})_m$  with *m* = integer can be prepared as single crystals from a  $\text{K}_2\text{MoO}_4$  flux or as nearly phase pure powders in sealed Pt tubes. The structural characteristics of the here prepared compounds agree with known compounds with general formula  $\text{AR}_3(\text{ZnO})_m$ , where A, R = trivalent metal and *m* = integer. Structural data from single crystal or powder X-ray diffraction have been published for only few of the homologous compounds, and to date any attempts to find an ordering of the R cation within the wurtzite region failed

1  
2 [16]. For the first time, the structure of  $\text{InGaO}_3(\text{ZnO})_2$  from  
3 single crystal data clearly shows an ordering of the R cation  
4 being  $\text{Ga}^{3+}$  which occupies the inversion boundary. This was  
5 proven by bond valence calculations as well. The same  
6 characteristic is observed for  $\text{InGaO}_3(\text{ZnO})_3$  from powder  
7 refinements and bond valence calculations as well, where  
8 tetrahedral sites close to the inversion boundary are  
9 occupied by the trivalent R cation. The tetrahedra in the  
10 wurtzite type region are increasingly deformed with  
11 decreasing distance to the inversion boundary, i.e. the  
12 cations shift from the tetrahedron centre towards the basal  
13 face the closer they are positioned to the inversion boundary.  
14 CBED techniques were used to doubtless determine the  
15 symmetry of the structure of the two compounds. Currently,  
16 pure compounds of members of the  $\text{InGaO}_3(\text{ZnO})_m$  family  
17 with  $m > 3$  are being prepared in our laboratory. In future  
18 work, the structures from single crystal data in combination  
19 with CBED and bond valence calculations shall be  
20 determined with focus on the cation distribution within the  
21  $(\text{Zn,Ga})\text{O}_4$  tetrahedra. In compounds with large  $m$  a different  
22 type of ordering and even formation of the unavoidable  
23 inversion boundary is expected [25, 26].  
24  
25  
26  
27  
28  
29  
30  
31  
32  
33  
34  
35  
36  
37  
38  
39  
40  
41  
42  
43  
44  
45  
46  
47  
48  
49  
50  
51  
52  
53  
54  
55  
56  
57  
58  
59  
60

1  
2  
3  
4  
5  
6 **Supporting Information** (see footnote on the first page of this  
7 article)

- 8  
9  
10  
11  
12  
13  
14  
15  
16  
17  
18  
19  
20  
21  
22  
23  
24  
25  
26  
27  
28  
29  
30  
31  
32  
33  
34  
35  
36  
37  
38  
39  
40  
41  
42  
43  
44  
45  
46  
47  
48  
49  
50  
51  
52  
53  
54  
55  
56  
57  
58
- [1] T. K. Gupta, *J. Am. Ceram. Soc.* **1990**, 73, 1817.  
[2] D. R. Clarke, *J. Am. Ceram. Soc.* **1999**, 82, 485.  
[3] D.G. Baik, S. M. Cho, *Thin Solid Films* **1999**, 354, 227.  
[4] G. Heiland, *Sensors and Actuators* **1982**, 2, 343.  
[5] A. Ghosh, S. Basu, *Mat. Chem. Phys.* **1991**, 27, 45.  
[6] Z. C. Jin, I. Hamberg, C. G. Granqvist, *Appl. Phys. Lett.* **1987**, 51, 149.  
[7] C. R. Gorla, N. W. Emanteoglu, S. Lg, W. E. Mayo, Y. Lu, M. Wraback, H. Shen, *J. Appl. Phys. Lett.* **1987**, 51, 149.  
[8] H. Ozta, W-S. Seo, K. Koumoto, *J. Am. Ceram. Soc.* **1996**, 79, 2193.  
[9] M. Nakamura, N. Kimizukka, T. Mohri, *J. Solid State Chem.* **1991**, 93, 298.  
[10] M. Nakamura, N. Kimizuka, T. Mohri, *J. Solid State Chem.* **1989**, 81, 70.  
[11] M. Nakamura, N. Kimizuka, T. Mohri, M. Isobe, *J. Solid State Chem.* **1993**, 103, 394.  
[12] C. Li, Y. Bando, M. Nakamura, N. Kimizuka, M. Onoda, *J. Solid State Chem.* **1998**, 139, 347.  
[13] M. Nakamura, N. Kimizuka, T. Mohri, M. Isobe, *J. Solid State Chem.* **1993**, 105, 535.  
[14] K. Kato, I. Kawada, N. Kimizuka, T. Katsura, *Z. Krist.* **1975**, 141, 314.  
[15] F. Lappe, A. Niggli, R. Nitsche, J. White, *Z. Krist.* **1962**, 117, 146.  
[16] M. Isobe, N. Kimizuka, M. Nakamura, T. Mohri, *Acta Cryst.* **1994**, C50, 332.  
[17] M. Nespolo, A. Sato, T. Osawa, H. Ohashi, *Cryst. Res. Technol.* **2000**, 35, 151.  
[18] J. P. Morniroli, J. W. Steeds, *Ultramicroscopy* **1992**, 45, 219.  
[19] A. Magrez, J. P. Morniroli, M. Caldes, A. Marie, O. Joubert, L. Brohan, *J. Of Solid State Chem.* **2003**, 172, 243.  
[20] P. A. Stadelmann, *Ultramicroscopy* **1987**, 21, 131.  
[21] G. M. Sheldrick, *Acta Cryst.* **2008**, A64, 112.  
[22] S. Boudin, K.-H.Lii, *Acta Cryst.* **1998**, C54, 5.  
[23] S. Adams, *St. Acta Cryst* **2001**, B57, 287.  
[24] <http://kristall.uni-mki.gwdg.de/softbv/index.html>.  
[25] E. D. T. Kamga, *Dissertation*, Friedrich-Wilhelms-Universität Bonn, **2008**.  
[26] F. Wolf, *Dissertation*, Friedrich-Wilhelms-Universität Bonn, **2003**.  
[27] Further details of the crystal structure investigation are available from the Fachinformationszentrum Karlsruhe, 76344 Eggenstein-Leopoldshafen, Germany (Fax: +49-7247-808666, E-Mail: [crysdata@fiz-karlsruhe.de](mailto:crysdata@fiz-karlsruhe.de)) referring to no. CSD-380305 (InGaO5Zn2), name of the authors and citation of the paper.

59 Received: ((will be filled in by the editorial staff))  
60 Published online: ((will be filled in by the editorial staff))

1  
2  
3  
4  
5  
6  
7  
8  
9  
10  
11  
12  
13  
14  
15  
16  
17  
18  
19  
20  
21  
22  
23  
24  
25  
26  
27  
28  
29  
30  
31  
32  
33  
34  
35  
36  
37  
38  
39  
40  
41  
42  
43  
44  
45  
46  
47  
48  
49  
50  
51  
52  
53  
54  
55  
56  
57  
58  
59  
60